Cerebral Cortex 2006;16:i138–i151
doi:10.1093/cercor/bhj168

A Role for Proneural Genes in the Maturation of Cortical Progenitor Cells

Olivier Britz[1,3], Pierre Mattar[2], Laurent Nguyen[1], Lisa-Marie Langevin[2], Céline Zimmer[1], Sharmila Alam[2], François Guillemot[1] and Carol Schuurmans[2]

[1]Division of Molecular Neurobiology, National Institute for Medical Research, The Ridgeway, Mill Hill, London, UK and [2]Department of Biochemistry and Molecular Biology, Institute of Maternal and Child Health, University of Calgary, Calgary, Alberta, Canada
[3]Current address: Molecular Neurobiology Laboratory, The Salk Institute for Biological Studies, La Jolla, CA 92037, USA

Olivier Britz and Pierre Mattar have contributed equally to this work. The two senior authors, François Guillemot and Carol Schuurmans, have contributed equally to this work.

We showed previously that the proneural genes *Neurogenin1 (Ngn1)* and *Ngn2* are required to specify the phenotypes of early- and not late-born neurons in the neocortex, acting in part through repression of *Mash1*, a third cortically expressed proneural gene. The precise timing of *Ngn1/2* specification activity was unexpected given these genes are expressed throughout cortical development, prompting us to search for a later function. Here we reveal that Ngn2 and Mash1 are expressed in a dynamic fashion, acquiring a cell cycle–biased, nonoverlapping distribution, with preferential expression in prospective basal progenitors, during mid corticogenesis. We also identified a new function for *Ngn2* during this latter period, demonstrating that it is required to regulate the transit of cortical progenitors from the ventricular zone (VZ) to the subventricular zone. Notably, *Ngn2* regulates progenitor maturation at least in part through repression of *Mash1* as misexpression of *Mash1* strongly enhanced progenitor cell exit from the VZ. Significantly, the ability of *Mash1* to promote progenitor cell maturation occurred independently of its ability to respecify cortical cells and is thus a novel function for *Mash1*. Taken together, these data support a model whereby *Ngn2* and *Mash1* function together to regulate the zonal distribution of progenitors in the developing neocortex.

Keywords: apical progenitors, basal progenitors, neocortex, proneural genes, subventricular zone

Introduction

In mouse, neocortical neurons are generated over a series of 11 progenitor cell divisions between embryonic day (E) 10 and E17 (Caviness 1982; Caviness and others 1995; Takahashi and others 1999). Radial glial cells are prototypical neural progenitors throughout the developing central nervous system (Noctor and others 2001; Malatesta and others 2003; Anthony and others 2004), including the neocortex, where they form a primary neurogenic zone in the ventricular zone (VZ) of the dorsal telencephalon (Kriegstein and Noctor 2004). During cell division, radial glia undergo specialized interkinetic nuclear movements that result in M-phase nuclei accumulating at the ventricular (apical) surface, whereas nuclei in S-phase form an abventricular band at the superficial margin or basal surface of the neuroepithelium (Sauer and Walker 1959). Slightly later in development, beginning from as early as E10.5 in lateral domains of the neocortex, a secondary pool of progenitors leaves the VZ to establish a more superficial subventricular zone (SVZ) (Ishii and others 2000; Brazel and others 2003; Haubensak and others 2004; Zimmer and others 2004). The SVZ or basal progenitors differ from radial glia in that they do not undergo interkinetic nuclear migration, they are not radially polarized, and they do not make contact with the ventricular surface (Haubensak and others 2004; Miyata and others 2004; Noctor and others 2004). Thus, whereas VZ (apical) progenitors undergo mitoses at the ventricular surface, SVZ progenitors undergo nonsurface mitoses.

Until recently, the prevailing view had been that VZ radial glia give rise to neurons (Sidman and others 1959; Bayer and others 1991), whereas SVZ progenitors primarily give rise to glia (Levison and Goldman 1993; Zerlin and others 1995; Kakita and Goldman 1999) and a limited number and type of neurons (Reynolds and Weiss 1992; Lois and Alvarez-Buylla 1993; Chiasson and others 1999). However, it had also been postulated early on that SVZ progenitors might also differentiate into upper layer cortical neurons (layers II–IV; Sidman and Rakic 1973; Smart and McSherry 1982; Smart and others 2002). In support of this idea, there is a correlation between markers that label the VZ and lower cortical plate (CP) neurons and the SVZ and upper CP neurons (Tarabykin and others 2001; Zimmer and others 2004). Moreover, cortical SVZ progenitors have been observed to predominantly undergo symmetric, neurogenic divisions during mid- to late corticogenesis (Haubensak and others 2004; Miyata and others 2004; Noctor and others 2004), lending support to the hypothesis that upper layer neurons are generated from secondary neurogenic divisions within the SVZ.

The molecular mechanisms that instruct VZ progenitors to produce SVZ progenitors are just beginning to be elucidated. In the ventral telencephalon, the proneural gene *Mash1*, encoding a basic-helix-loop-helix (bHLH) transcription factor, is required to prevent the precocious acquisition of SVZ properties by VZ progenitors (Casarosa and others 1999; Yun and others 2002). *Mash1* has also been implicated in the differentiation of early- and not late-born neurons in the striatum, indicating that this gene regulates both progenitor cell behavior and neuronal fate specification in a temporally defined manner (Casarosa and others 1999; Yun and others 2002). Similarly, in the neocortex, we have shown that the proneural bHLH genes *Neurogenin1* (*Ngn1*) and *Ngn2* are absolutely required to specify the identities of early born, deep-layer neurons, whereas they are dispensable for later stages of neuronal fate specification (Schuurmans and others 2004). Gain-of-function studies have also suggested that *Ngn2* promotes nonsurface cell divisions that expand the cortical

SVZ (Miyata and others 2004). Taken together, these studies suggest that proneural genes may coordinate progenitor cell maturation and neuronal fate specification events during telencephalic development.

To examine further whether proneural genes control progenitor cell behavior in the neocortex, we performed a series of loss- and gain-of-function studies. We focused on *Ngn1* and *Ngn2*, which are expressed at high levels in cortical progenitors, as well as *Mash1*, a proneural gene that we found to be expressed in dorsal telencephalic progenitors, albeit at lower levels than in ventral telencephalic domains. We found that the expression profiles of the proneural proteins underwent a striking transition from early to intermediate stages of cortical development, acquiring a segregated, zonal distribution and cell cycle bias that was not initially apparent. The segregated expression of the proneural proteins in the E15.5 VZ led us to consider their potential role in the maturation of cortical progenitors. Strikingly, in mid stage (E15.5) *Ngn2* and *Ngn1;Ngn2* mutants, an increased proportion of dividing cells accumulated in the SVZ and intermediate zone (IZ) at the expense of the VZ. We also observed that ectopic expression of *Mash1*, which we previously reported to be upregulated in *Ngn* mutants (Fode and others 2000), was most evident in the SVZ and IZ. Consistent with the idea that the ectopic expression of *Mash1* accelerated the movement of *Ngn* mutant cortical cells, *Mash1* misexpression rapidly promoted the exit of wild-type cells from the VZ to the SVZ/IZ. Notably, although *Mash1* misexpression was able to ventralize early cortical progenitors, it did not change the fate of mid stage progenitors, indicating that the induction of progenitor cell maturation and migration occurred independently of the conversion of cell fates. Taken together, these results demonstrate that the proneural genes independently regulate neuronal fate specification and progenitor cell maturation.

Materials and Methods

Animals

Embryos were staged using the morning of the vaginal plug as E0.5. $Ngn2^{GFPKI}$ mutant lines were maintained as heterozygotes on a CD1 background, and genotyping was performed using 30 cycles of 94 °C/min, 60 °C/min, 72 °C/min and the following primers for wild-type (VC176 + VD187) and $Ngn2^{GFPKI}$ mutant alleles (VD187 + ZF92). VC176: AGATGTAATTGTGGGCGAAG; VD187: GGACATTCCCGGACACACAC; ZF92: GCATCACCTTCACCCTCTCC. *Mash1* and *Ngn1* mutants were genotyped as described (Ma and others 1998; Casarosa and others 1999). CD1 mice (Charles River) were used for in utero electroporation experiments.

Mash1 Expression Construct and In Utero Electroporation

Mash1 cDNA was amplified by polymerase chain reaction and subcloned into a pCIG2 expression vector obtained from Franck Polleux (Hand and others 2005). In this vector, *Mash1* was subcloned 3′ of a recombinant β-actin enhancer/cytomegalovirus promoter element and 5′ of an internal ribosome entry site (IRES)-enhanced green fluorescent protein reporter cassette. Endotoxin-free plasmid DNA was prepared for electroporation using a column-based purification system (Qiagen, Mississauga, Ontario, Canada). In utero electroporation was performed essentially as described (Saito and Nakatsuji 2001). Briefly, uteri of anesthetized pregnant mothers were exposed through an incision in the ventral peritoneum. DNA (3 μg/μl) was injected through the uterine wall into the telencephalic vesicle using pulled borosilicate needles and a Femtojet microinjector (Eppendorf, Mississauga, Ontario, Canada). Five pulses of 40–60 mV were applied across the uterine wall at 400-ms intervals using 5-mm platinum tweezer-style electrodes (Protech, San Antonio, TX) and a BTX square wave electroporator (VWR CanLab, Mississauga, Ontario, Canada). The uterus was then replaced in the abdominal cavity, and embryonic development proceeded as normal.

Tissue Processing

Embryonic brains were dissected in 1× phosphate-buffered saline (PBS) and fixed for 30 min to 2 h (for immunohistochemistry) or overnight (for RNA in situ hybridization) in 4% paraformaldehyde (PFA)/1× PBS at 4 °C. Fixed brains were cryoprotected overnight in 20% sucrose/1× PBS at 4 °C and then blocked in optimal cutting temperature (Tissue-Tek) compound and frozen on dry ice. Brains were sectioned using a cryostat at 10 μm.

RNA In Situ Hybridization

RNA in situ hybridization was performed using digoxygenin (dig)-labeled probes as described previously (Cau and others 1997). The templates used to generate probes included: *Mash1* (Cau and others 1997), *Ngn2* (Gradwohl and others 1996), *Ngn1* (Ma and others 1997), *Dlx1* (Anderson and others 1997), *Cux2* (Nieto and others 2004), *Sema3C*, *Unc5b4, Id4* (Mattar and others 2004), *EGFP* (cloned enhanced green fluorescent protein [EGFP] coding sequence from pEGFP [Clontech] into pBluescript SK [Stratagene]), *NeuroD* (Miyata and others 1999), *Delta1* (Lindsell and others 1996), *GAD1* (Behar and others 1994), and *Pax6* (Stoykova and others 2000).

Immunohistochemistry

Cryostat sections were blocked for 1 h at room temperature in 3% bovine serum albumin/1× TBST (Tris-Buffered Saline: 25 mM Tris, 0.14 M NaCl, 0.1% Triton X-100) or 10% normal goat serum/1× PBST. Primary antibodies were diluted in blocking solution and applied for 2 h at room temperature or overnight at 4 °C. Sections were washed 4 times for 10 min in TBS, and secondary antibodies were applied for 2 h in blocking solution. Sections were washed 4 times for 10 min in TBST, nuclei were counterstained with 4',6-diamidino-2-phenylindole, dihydrochloride (1/10000, Sigma, Oakville, Ontario, Canada) or with Toto3 (1/1000, Molecular Probes, Eugene, OR), washed 4 times for 10 min in TBST, and mounted using AquaPolymount (Polysciences Inc., Warrington, PA). For 5-bromo-2-deoxyuridine (BrdU) incorporation experiments, pregnant mothers were injected intraperitoneally with 100-μg/g body weight of BrdU (Sigma). For immunohistochemical detection of BrdU, sections were denatured in 2 N HCl for 30 min at 37 °C, neutralized in 0.1 M borate buffer pH 8.5, rinsed with PBS, and blocked and stained as above. For Ngn2/BrdU, Mash1/BrdU, and Ki67/BrdU coimmunohistochemistry, labeling for Ngn2, Mash1, and Ki67 was completed first, followed by postfixation in 4% PFA/1× PBS for 10 min at room temperature. Sections were then denatured and processed for BrdU immunohistochemistry as above. Primary antibodies included: mouse anti-Mash1 (1/100, BD Biosciences, Mississauga, Ontario, Canada), mouse anti-Ngn2 (1/20, gift from David Anderson), rabbit anti-Ngn1 (1/500, gift from Jane Johnson), mouse anti-BrdU (1/100, Roche, Mississauga, Ontario, Canada), rat anti-BrdU (1/20, ImmunologicalsDirect), rabbit anti-phosphohistone H3 (pHH3) (1/1000, Upstate Biotechnology, Charlottesville, VA), rabbit anti-Pax6 (1/500, Babco), polyclonal pan-Dll antibody (1/500, gift from Grace Panganiban), rat anti-Ki67 (1/50, clone TEC3, Dako, Mississauga, Ontario, Canada), mouse anti-neuronal class β III-Tubulin (TuJ1) (1/1000, Babco), rabbit anti β III-tubulin (1/1000, Babco), rabbit anti-GFP (1/500, Chemicon, Temecula, CA) and anti-NeuN (1/500, Chemicon). Secondary antibodies were conjugated to Alexa488 or Alexa568 (Molecular Probes), Cy3 or Cy5 (Jackson Immunoresearch: West Grove, PA).

Quantification and Statistics

Cells immunopositive for different markers were quantified in photomicrographs of the dorsomedial cortex, focusing on rostral sections at the level of the striatum. Cells were counted in a minimum of 3 sections taken from each embryo. The numbers of wild-type and mutant embryos used in each experiment are indicated in the text. Statistical significance was calculated using Student's *t*-test for pairwise comparisons or analysis of variance + Tukey's for multiple comparisons.

Results

Ngn2 and Mash1 Are Differentially Expressed in Cortical Progenitors

We previously showed that the 3 proneural genes, *Ngn1*, *Ngn2*, and *Mash1*, are expressed in the developing cerebral cortex,

where they are required for the neuronal commitment of progenitors and to specify the cortical regional identity and neurotransmission phenotype of early born neurons (Fode and others 2000; Nieto and others 2001; Schuurmans and others 2004). The proneural genes function in this capacity only during early phases of corticogenesis, despite their continuous expression, raising the possibility of a distinct role for these genes at later stages. To gain a better understanding of how the proneural genes might function during mid–late corticogenesis, we questioned whether a change in their cellular distribution might underlie temporal differences in their function.

We first examined the cortical expression of proneural proteins at E12.5, corresponding to the *Ngn*-dependent phase of neuronal specification. At E12.5, the dorsal telencephalon consists of a VZ, where proliferating progenitors are located, and a preplate layer, containing the earliest born cortical neurons. Using proneural-specific antisera, we showed that at this stage, only a small fraction of randomly distributed cortical nuclei in the VZ expressed detectable levels of Mash1 (11.6 ± 4.8%, $n = 6$; Fig. 1*A*), Ngn1 (6.7 ± 1.1%, $n = 4$; Fig. 1*B*), and Ngn2 (10.0 ± 4.7%, $n = 4$; Fig. 1*C*) proteins. In double-labeling experiments, Ngn1 was almost entirely coexpressed with Ngn2 (95% Ngn1-positive progenitors coexpressed Ngn2; Fig. 1*J*), consistent with the genetic redundancy of these 2 genes. Moreover, many Mash1-positive nuclei expressed Ngn1 (39.9 ± 4.8%, $n = 4$; Fig. 1*K*) and Ngn2 (33.9 ± 12.2%, $n = 3$; Fig. 1*L*), whereas reciprocally, a large percentage of Ngn1 (39.9 ± 13.7%, $n = 4$) and Ngn2 (55.7 ± 5.6%, $n = 3$) expressing progenitors were also Mash1 positive (Fig. 1*K,L*). Thus, at this early stage, when only a small fraction of cortical progenitors have begun to express detectable levels of the proneural proteins, the Ngns and Mash1 are coexpressed to a large extent.

We next examined proneural expression at E15.5, a stage when a SVZ containing nonsurface dividing or basal progenitors has become histologically distinguishable. At this stage, we noted a striking change in the overall distribution of Mash1-, Ngn1-, and Ngn2-expressing nuclei. First, Mash1-expressing nuclei preferentially accumulated in 2 sectors in the VZ, one near the ventricular surface and a second at the VZ/SVZ border, with some Mash1-expressing nuclei also scattered throughout the SVZ and IZ (Fig. 1*D*). This pattern was mirrored by a similarly segregated distribution of *Mash1* transcripts in the E15.5 neocortex, which were present at notably lower levels in the central VZ (Fig. 1*G*). In contrast, the majority of nuclei containing Ngn1 (Fig. 1*E*) and Ngn2 (Fig. 1*F*) proteins were present in the central region of the VZ and were less abundant near the ventricular surface and at the VZ/SVZ border. The distribution of *Ngn1* (Fig. 1*H*) and *Ngn2* (Fig. 1*I*) transcripts faithfully recapitulated the protein expression profiles. Consistent with their apparently nonoverlapping expression domains, the level of Ngn2 and Mash1 coexpression in the VZ dropped substantially at E15.5 as compared with E12.5 (11.4 ± 6.7% Ngn2+ nuclei also Mash1+ and 19.7 ± 7.5% Mash1+ nuclei also Ngn2+), whereas remaining slightly higher in the SVZ (23.8 ± 10.7% Ngn2+ nuclei also Mash1+ and 34.6 ± 6.7% Mash1+ nuclei also Ngn2+; Fig. 1*M–O*). Mash1 and Ngn2 thus acquire largely exclusive expression domains in the cortical VZ by E15.5.

Ngn2 and Mash1 Are Preferentially Expressed in Distinct Phases of the Cell Cycle in Mid Stage Cortical Progenitors

VZ progenitors undergo interkinetic nuclear migration in a cell cycle–related manner (Sauer and Walker 1959). The zonal distribution of the proneural-expressing nuclei in the E15.5 VZ was thus highly suggestive of cell cycle regulation. We therefore examined whether Mash1 and Ngn2 expression was indeed restricted to a specific phase of the cell cycle. We did not further examine Ngn1, as it was highly coexpressed with Ngn2 and has no detectable function in corticogenesis on its own (Schuurmans and others 2004).

To label cortical progenitors in a particular phase of the cell cycle, we performed a series of BrdU pulse–labeling

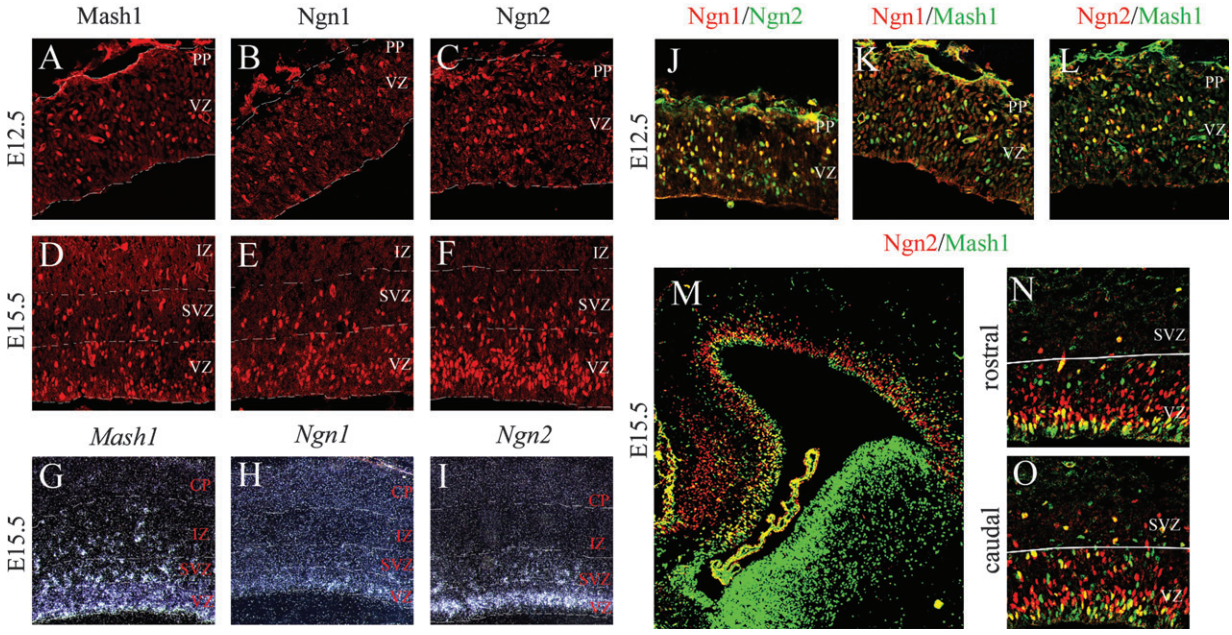

Figure 1. Dynamic expression of Mash1, Ngn1, and Ngn2 in early and mid stage cortical progenitors. Expression of Mash1 (*A*), Ngn1 (*B*), and Ngn2 (*C*) protein in E12.5 cortices. Expression of Mash1 (*D*), Ngn1 (*E*), and Ngn2 (*F*) protein in E15.5 cortical progenitors. Distribution of *Mash1* (*G*), *Ngn1* (*H*), and *Ngn2* (*I*) transcripts in the E15.5 neocortex. Double immunolabeling of Ngn1/Ngn2 (*J*), Ngn1/Mash1 (*K*), and Ngn2/Mash1 (*L*) at E12.5 and of Ngn2/Mash1 (*M–O*) at E15.5. PP, preplate.

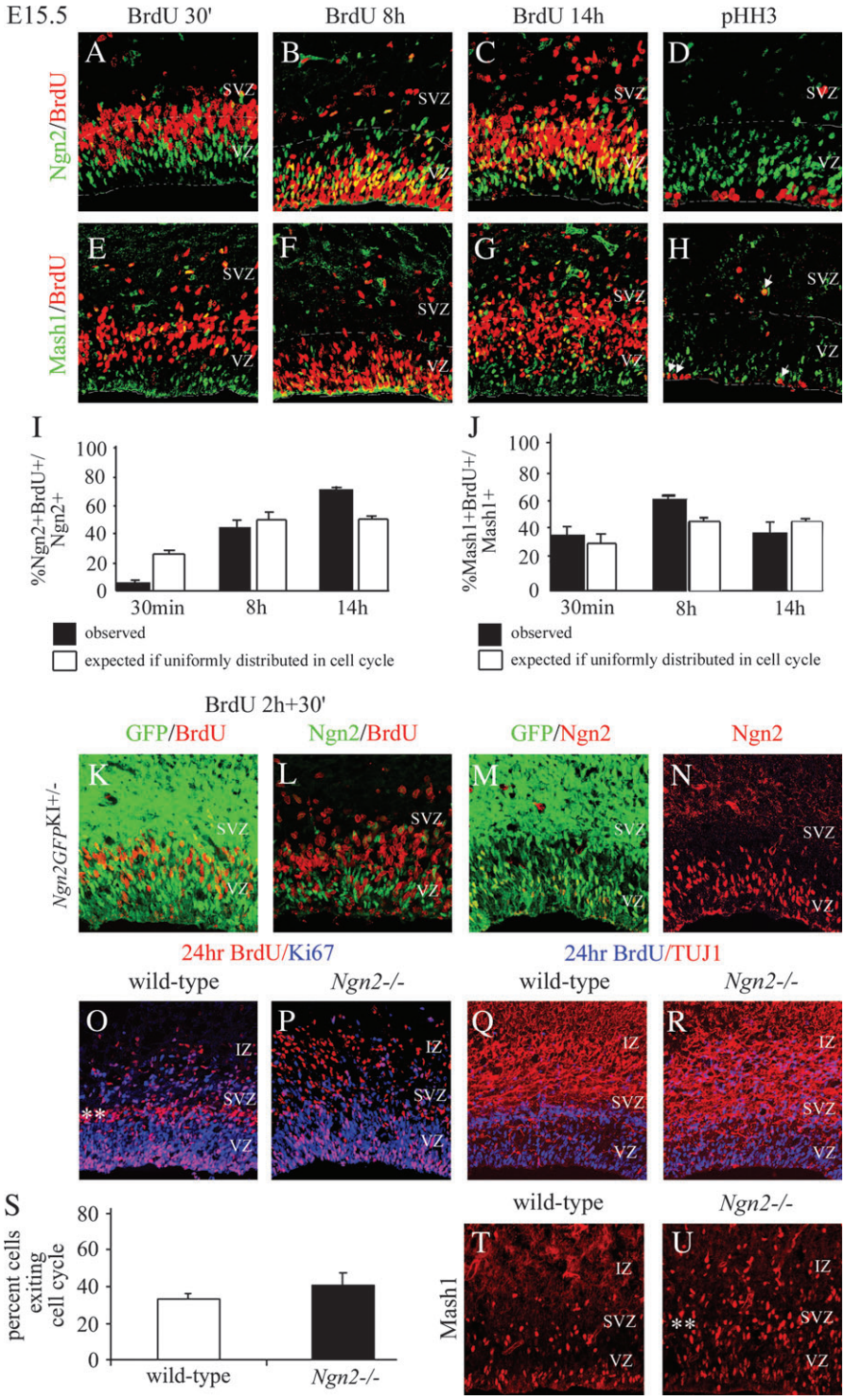

Figure 2. Ngn2 and Mash1 are expressed in a cell cycle–biased fashion in future basal progenitors in the E15.5 cortical VZ. E15.5 embryos were labeled with BrdU for 30 min to mark cells in S-phase (*A*, *E*), 8 h to mark cells in early-to-mid G1 (*B*, *F*), and 14 h to mark cells in late G1 (*C*, *G*), prior to harvesting. Cortical sections were then stained with anti-Ngn2 and anti-BrdU (*A–C*) or with anti-Mash1 and anti-BrdU (*E–G*). E15.5 cortical sections were also immunolabeled with anti-Ngn2 and anti-pHH3 (*D*) or anti-Mash1 and anti-pHH3 (*H*). (*I*) Quantification of Ngn2/BrdU double-positive cells as a ratio of the entire Ngn2-positive population in the VZ following different BrdU pulse lengths (filled bars) compared with the proportion of BrdU-labeled cells in the VZ (open bars). (*J*) Quantification of Mash1/BrdU double-positive cells as a ratio of the entire Mash1-positive population following different BrdU pulse lengths. (*I*, *J*) Black bars represent the observed ratio, and white bars are the percentage of cells expected with a random distribution in the cell cycle. E15.5 *Ngn2*$^{GFP\text{KI}}$ heterozygotes pulse labeled with BrdU 2 h and again at 30 min prior to immunostaining with GFP/BrdU (*K*), Ngn2/BrdU (*L*), and GFP/Ngn2 (*M*, *N*). (*O*, *P*) Immunolabeling of E15.5 wild-type (*O*) and *Ngn2* mutant (*P*) cortices with anti-Ki67 (blue) and anti-BrdU (red). Embryos received a BrdU pulse 24 h prior to harvesting. Asterisks denote the accumulation of BrdU-positive/Ki67-negative cells that had exited the cell cycle at the border between the VZ and SVZ in wild-type embryos (*O*). (*Q*, *R*) Immunolabeling of E15.5 wild-type (*Q*) and *Ngn2* mutant (*R*) cortices with anti-TUJ1 (red) and anti-BrdU (blue) to label postmitotic cells that had differentiated into neurons over 24 h. (*S*) Quantification of the Q- or leaving fraction, representing the total number of BrdU-positive, Ki67-negative cells that had exited the cell cycle in E15.5 wild-type versus *Ngn2* mutants. (*T*, *U*) Immunostaining of E15.5 wild-type (*T*) and *Ngn2* mutant (*U*) cortical sections with anti-Mash1. Asterisks in (*U*) show an increase in Mash1-expressing cells at the VZ/SVZ border in *Ngn2* mutants.

experiments, as well as immunostaining with anti-pHH3, a late G2/M-phase marker (Weissman and others 2003). First, to label S-phase progenitors, E15.5 embryos were exposed to BrdU 30 min prior to harvesting. S-phase nuclei marked with anti-BrdU were distributed in an abventricular band at the top of the VZ, as expected from their interkinetic nuclear movements (Fig. 2*A,E*). In colabeling experiments with anti-Ngn2, the percentage of Ngn2/BrdU double-positive progenitors was only 5.4 ± 1.5% of the total Ngn2+ population, a fraction well below the proportion of Ngn2-positive progenitors expected to be in S-phase if Ngn2 was homogeneously expressed throughout the cell cycle (25.4 ± 2.0% of VZ cells labeled by $BrdU_{30'}$, $P < 0.01$, $n = 3$; Fig. 2*A,I*). To examine Ngn2 expression during both S-phase and G2/M-phases of the cell cycle, we performed 2 successive injections of BrdU, one 2 h prior to sacrifice and a second 30 min before harvesting, resulting in a cumulative labeling of S/G2/M-phase progenitors (Fig. 2*L*). In these experiments, 10 ± 3.9% of Ngn2-positive cells colabeled with anti-BrdU, compared with an expected 36.4 ± 3.2% (fraction of BrdU+ cells among all VZ cells, $P < 0.03$, $n = 3$), if Ngn2 was homogeneously expressed throughout the cell cycle. Moreover, consistent with an exclusion from G2/M-phase of the cell cycle, only occasional Ngn2-positive nuclei were colabeled by anti-pHH3 (Fig. 2*D*).

By changing BrdU pulse times, we next examined the distribution of Ngn2-expressing nuclei in G1-phase of the cell cycle. At E15.5, the cell cycle is 18 h in length, including a 12-h G1-phase, 4-h S-phase, and 2-h G2/M-phase (Takahashi and others 1995). To label nuclei in early-to-mid G1, E15.5 embryos were subjected to a single pulse of BrdU 8 h prior to harvesting, whereas labeling of late G1 was achieved by collecting embryos 14 h after BrdU injection. Double immunolabeling of embryos subjected to an 8-h BrdU pulse with anti-BrdU and anti-Ngn2 revealed that 43.9 ± 5.6% of the Ngn2-expressing nuclei incorporated BrdU, similar to the proportion of 49.6 ± 6.2% expected if Ngn2 was randomly expressed throughout the cell cycle, suggesting a lack of enrichment during early G1 ($n = 3$, Fig. 2*B,I*). However, a significantly larger fraction of the Ngn2-positive cohort colabeled with BrdU after a 14-h pulse (70.3 ± 0.9%) as compared with that expected from a random distribution of Ngn2+ nuclei through the cell cycle (50.9 ± 1.8%, $P < 0.001$, $n = 3$; Fig. 2*C,I*). There was therefore a bias toward Ngn2 being expressed in cycling progenitors in the latter portion of G1 and/or in cells that had exited the cell cycle and entered G0. Of note, using a different methodology, another group also concluded that Ngn2 is enriched in cells in G1 (Miyata and others 2004).

Similar experiments were performed with Mash1. In E15.5 embryos subjected to a BrdU pulse 30 min prior to harvesting, the percentage of Mash1-positive nuclei also labeled by BrdU (36.4 ± 6.8%) was not significantly different from the ratio expected for a random cell-cycle distribution (32.0 ± 5.2%, $n = 3$; Fig. 2*E,J*), in contrast to what had been observed for Ngn2. Mash1 was also expressed in some pHH3+ nuclei, consistent with the idea that it was not excluded from G2/M-phase of the cell cycle (Fig. 2*H*). However, when embryos were collected 8 h after the BrdU pulse, considerably more Mash1-positive cells were colabeled with BrdU (61.4 ± 1.8%) than expected from a random cell-cycle distribution (46.7 ± 1.7%, $P < 0.02$, $n = 3$; Fig. 2*F,J*), suggesting that Mash1 was enriched in early–G1-phase cells. Moreover there was a trend toward fewer Mash1-positive cells labeled with BrdU after 14 h (38.8 ± 7.0%) than would be expected if Mash1 was indiscriminately expressed throughout the cell cycle (45.6 ± 1.6%, $n = 3$; Fig. 2*G,J*). Thus, Mash1 preferentially accumulates in early G1-phase, whereas Ngn2 accumulates later in this phase of the cell cycle. Taken together, these observations were consistent with Mash1 and Ngn2 acquiring complementary expression domains by E15.5.

Ngn2 Is Expressed by VZ Cells on Their Way to the SVZ

VZ progenitors at mid corticogenesis are radial glial cells that primarily divide asymmetrically, generating either a VZ progenitor/radial glial cell and a neuron or a VZ radial glial cell and a progenitor that divides symmetrically in a basal position. A much smaller fraction of VZ progenitors divides symmetrically to generate 2 radial glial cells (Haubensak and others 2004; Miyata and others 2004; Noctor and others 2004). The restricted distribution of Ngn2 in the VZ to nuclei in the latter portion of G1- and/or G0-phase may correspond to basal progenitors or postmitotic neurons on their way to the SVZ. Alternatively, Ngn2 may be expressed by radial glial cells that are entering a new cell cycle in the VZ. To examine whether Ngn2 was preferentially expressed in cells leaving the VZ versus a cyclical expression in progenitors that continued to divide in the VZ, we took advantage of EGFP as a short-term lineage tracer in our $Ngn2^{EGFPKI}$ line (Seibt and others 2003). For this, cortices from E15.5 $Ngn2^{EGFPKI}$ heterozygotes, in which S/G2/M-phase progenitors were labeled by BrdU injections 2 h and 30 min prior to sacrifice, were immunolabeled with anti-GFP and anti-BrdU. In these experiments, GFP-expressing cells were for the most part BrdU negative in the VZ (9.5 ± 4.9% double positive vs. 31.2 ± 11.1% expected if GFP were expressed in S-phase; $P = 0.09$, $n = 2$; Fig. 2*K*), as was Ngn2 (Fig. 2*L*; see above), indicating that, like Ngn2, GFP is induced in VZ cells mostly after they have left the S/G2/M-phases. Given GFP stability, this indicates that GFP, and therefore Ngn2, is not expressed in cells that self-renew in the VZ, but only in cells that leave the VZ after the G1/G0-phase. Moreover, GFP was largely coexpressed with Ngn2 in VZ cells (Fig. 2*M,N*), which would not be expected if Ngn2 was expressed in cycling G1 cells and transiently downregulated in S/G2/M. Instead, the vast majority of SVZ cells were GFP positive in E15.5 $Ngn2^{EGFPKI}$ heterozygote cortices (Fig. 2*K,M*). These results thus indicate that VZ progenitors rapidly migrate into the SVZ after initiating the expression of Ngn2, confirming that Ngn2 is primarily expressed in future basal progenitors and/or in newly differentiated neurons rather than in self-renewing VZ progenitors.

Increase in Basal at the Expense of Apical Cell Divisions in Ngn2 and Ngn1/Ngn2 Mutants

We reasoned that the distinct distribution of Ngn2 and Mash1 in VZ cells could reflect distinct roles for these proteins in regulating the progression of cortical progenitors from the VZ to SVZ. To address this possibility, we performed a qualitative and quantitative assessment of dividing progenitors in *Mash1*, *Ngn1*, and *Ngn2* mutant cortices with a series of BrdU pulses at E15.5. First, to ensure that interkinetic nuclear migration was not perturbed in any of the mutant backgrounds, pregnant dams were subjected to a 30-min BrdU pulse prior to sacrifice. In E15.5 wild-type, *Mash1*, *Ngn1*, and *Ngn2* mutant cortices, anti-BrdU immunostaining revealed a similar abventricular band of S-phase cells (Fig. 3*A–D*), indicating that the loss of a single proneural gene did not result in gross defects in nuclear migration.

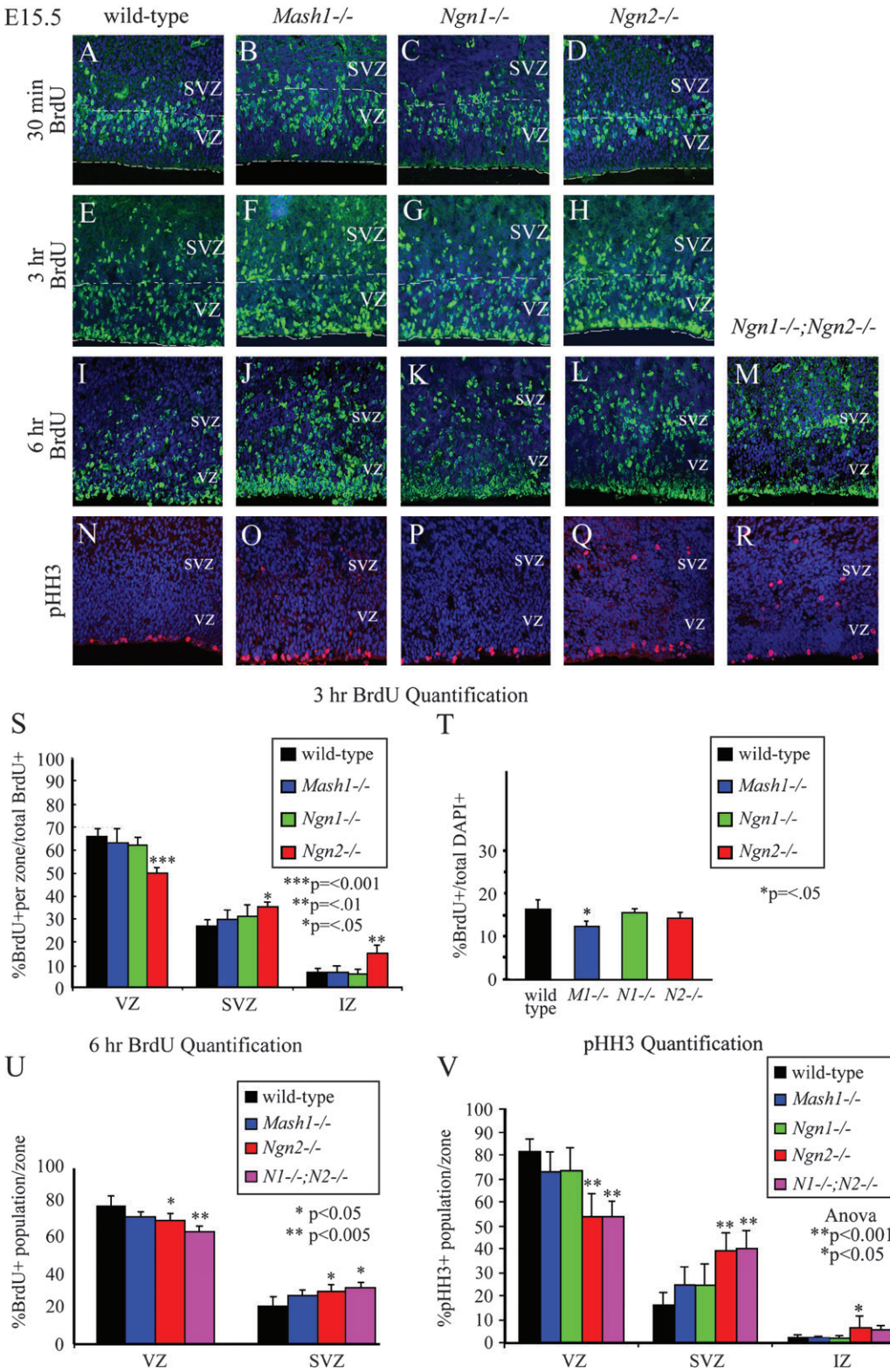

Figure 3. Reduction in proliferating apical progenitors in the VZ and expansion of the basal progenitor pool in the SVZ in *Ngn2* and *Ngn1;Ngn2* mutants. (*A–D*) E15.5 wild-type (*A*), *Mash1* mutant (*B*), *Ngn1* mutant (*C*), and *Ngn2* mutant (*D*) embryos were exposed to BrdU 30 min prior to harvesting. (*E–H*) E15.5 wild-type (*E*), *Mash1* mutant (*F*), *Ngn1* mutant (*G*), and *Ngn2* mutant (*H*) embryos were exposed to BrdU 3 h prior to harvesting. (*I–M*) E15.5 wild-type (*I*), *Mash1* mutant (*J*), *Ngn1* mutant (*K*), and *Ngn2* mutant (*L*) and *Ngn1;Ngn2* mutant (*M*) embryos were exposed to BrdU 6 h prior to harvesting. (*N–R*) E15.5 wild-type (*N*), *Mash1* mutant (*O*), *Ngn1* mutant (*P*), *Ngn2* mutant (*Q*), and *Ngn1;Ngn2* mutant (*R*) embryos immunolabeled with anti-pHH3. Sections were counterstained with DAPI to label nuclei (*A–R*). (*S*) Quantification of BrdU-positive nuclei in each zone as a percentage of the total BrdU-positive population. (*T*) Quantification of the total number of BrdU-positive nuclei as a percentage of the total number of DAPI-labeled nuclei. (*U*) Quantification of pHH3-positive nuclei in each zone as a percentage of the total pHH3-positive population. (*V*) Quantification of the percent of pHH3-positive nuclei per DAPI-labeled nuclei at the ventricular surface. Statistical significance was calculated with analysis of variance + Tukey's.

Next, E15.5 wild-type and proneural mutant embryos were subjected to a pulse of BrdU 3 h prior to harvesting, labeling G2/M-phase (near the ventricular surface) and S-phase (abventricular band) nuclei (Fig. 3*E–H*). BrdU-expressing cells were counted in each cortical zone and were represented as the percentage of the entire BrdU-labeled population. In wild-type embryos, 65.8 ± 3.6% labeled cells were present in the VZ, 27.1 ± 2.5% in the SVZ, and 7.2 ± 1.8% in the IZ ($n = 5$; Fig. 3*E,S*). In *Ngn2* mutants, a lower proportion of dividing cells were labeled in the VZ (49.7 ± 2.8%, $P < 0.001$, $n = 4$), whereas a larger fraction of dividing cells were present in the SVZ (35.2 ± 2.1%, $P < 0.05$) and IZ (15.1 ± 3.8%, $P < 0.01$, Fig. 3*H,S*). In contrast, no significant differences were observed in the proportions of dividing cells in each zone in *Mash1* ($n = 4$; Fig. 3*F,S*) or *Ngn1* ($n = 3$; Fig. 3*G,S*) single mutants. There was however a slight reduction in the overall number of BrdU-labeled DAPI-positive cells in *Mash1* single mutants (12.5 ± 1.2% in *Mash1* mutants vs. 16.3 ± 2.1% in wild types; $P < 0.05$, $n = 4$ *Mash1* mutants and $n = 5$ wild type), whereas similar numbers of germinal zone cells were BrdU labeled in wild-type, *Ngn1*, and *Ngn2* mutant cortices (Fig. 3*T*). The loss of *Ngn2* thus resulted in an overall change in the position of progenitor cells (i.e., in VZ or SVZ compartments), whereas the loss of *Mash1* resulted in a slight decrease in the overall number of progenitors labeled post–S-phase, suggesting distinct roles for these factors in regulating the division of cortical progenitors.

We used 2 additional labeling methods to examine further the distribution of dividing cells in the VZ and SVZ of proneural mutant neocortices. First, we exposed E15.5 wild-type and proneural mutant embryos to a pulse of BrdU 6 h prior to harvesting, which served as a short-term birthdating experiment due to the rapid clearance of BrdU in vivo. In wild-type cortices, the majority of BrdU-labeled nuclei accumulated in the lower half of the VZ (i.e., in G2/M and early G1), whereas fewer labeled cells were present in the upper VZ, where S-phase nuclei are located (Fig. 3*I*). The reduction in BrdU-positive S-phase nuclei in the VZ provided a clearer delineation between the SVZ and VZ than in previous experiments with shorter harvest times following the BrdU pulse. In *Mash1* single mutant embryos ($n = 3$; Fig. 3*J*), the distribution of BrdU-labeled cortical nuclei in the VZ and SVZ was similar to that of wild-type embryos ($n = 4$; Fig. 3*I,U*). However, in *Ngn2* single ($n = 5$; Fig. 3*L,U*) and *Ngn1;Ngn2* double ($n = 1$; Fig. 3*M,U*) mutant cortices, there was a significant increase in the number of BrdU-labeled nuclei in the SVZ compartment (29.6 ± 4.5%, $P < 0.003$ and 32.1 ± 2.8%, $P < 0.02$, respectively, compared with 21.2 ± 6.7% in wild-type cortices) and a parallel decrease in the VZ (70.4 ± 5.0%, $P < 0.003$ and 63.8 ± 3.0%, $P < 0.004$ in *Ngn2* single and *Ngn1;Ngn2* double mutants, respectively vs. 78.7 ± 6.7% in wild type).

To provide further support for the expansion of the proliferating population in the SVZ/IZ at the expense of the VZ in *Ngn* mutants, we next examined the distribution of pHH3-expressing mitotic nuclei in a larger set of E15.5 wild-type and proneural mutant cortices. In wild-type embryos at E15.5, 81.4 ± 5.8% ($n = 10$) of the pHH3-positive population was found in the VZ, whereas only 15.9 ± 5.7% of the pHH3-expressing nuclei were in the SVZ (Fig. 3*N,V*). In *Mash1* ($n = 6$; Fig. 3*O,V*) and *Ngn1* ($n = 6$; Fig. 3*P,V*) single mutants at the same stage, there was a slight trend toward fewer VZ and more SVZ mitotic nuclei, but these differences did not reach statistical significance. In contrast, there was a clear reduction in the number of mitotic nuclei in the VZ of *Ngn2* single (53.8 ± 10.0%; $P < 0.001$; $n = 9$; Fig. 3*Q,V*) and *Ngn1;Ngn2* double (54.0 ± 6.4%; $P < 0.001$; $n = 3$; Fig. 3*R,V*) mutant cortices as compared with wild type. The reduction in mitoses in the VZ was mirrored by a significant increase in the number of mitotic nuclei in the SVZ of *Ngn2* single (39.1 ± 7.7%; $P < 0.001$; $n = 9$) and *Ngn1;Ngn2* double (40.1 ± 7.8%; $P < 0.001$; $n = 3$) mutants and a trend toward more dividing cells in the IZ, which reached significance in *Ngn2* single mutants (6.6 ± 4.9% in *Ngn2* mutants vs. 2.5 ± 0.8% in wild type; $P < 0.05$; $n = 9$ *Ngn2* mutants and $n = 10$ wild type; Fig. 3*V*). Notably, *Ngn1;Ngn2* double mutants did not manifest any additive changes in progenitor distribution versus *Ngn2* single mutants (Fig. 3*R,V*), suggesting that *Ngn1* provides no genetic compensation for this function when *Ngn2* is lost.

Finally, we questioned whether the change in the VZ/SVZ ratio observed at E15.5 was already detectable at earlier stages of cortical development, when nonsurface cell divisions are already present although less prominent (Smart and McSherry 1982; Haubensak and others 2004). For this, we labeled wild-type and *Ngn2* mutant cortices at E12.5, E13.5, and E14.5 with anti-pHH3. There was no significant difference in the absolute number of mitotic nuclei or in the ratio of nuclei undergoing surface versus nonsurface mitoses in *Ngn2* mutant versus wild-type cortices at these 3 stages, although a trend toward a decrease in the ratio of surface/nonsurface division became apparent at E14.5 (data not shown). This suggested that the requirement for *Ngn2* to regulate the progression of VZ progenitors into the SVZ is restricted to mid–late stages of corticogenesis.

Neuronal Output Is Unchanged in the Ngn2 Mutant Cortex

Basal or nonsurface-dividing progenitors in the SVZ have recently been shown to preferentially divide symmetrically to give rise to 2 neurons, whereas radial glial cells in the VZ mostly divide asymmetrically, generating another radial glial cell and either a neuron or a basal progenitor (Haubensak and others 2004; Miyata and others 2004; Noctor and others 2004). Given the expansion of basal at the expense of apical progenitors in *Ngn2* mutants, we next set out to investigate whether there was a significant increase in neuronal output in these mutants. To quantify the leaving (Q)-fraction, we exposed E15.5 wild-type and *Ngn2* mutants to a pulse of BrdU 24 h prior to harvesting. All cells that were still proliferating were then identified using the Ki67 pan-proliferating marker (Fig. 2*O,P*), whereas cells that had initiated neuronal differentiation were identified with Neuronal Class III β-Tubulin an immature neuronal marker (Fig. 2*Q,R*). Cells that were dividing at the time of the BrdU pulse, but had subsequently undergone terminal mitosis and entered G0, were thus BrdU-positive, Ki67-negative, and TUJ1-positive. Quantification of BrdU-positive/Ki67-negative cells revealed that the percentage of cells exiting the cell cycle was not significantly altered in *Ngn2* mutant as compared with wild-type cortices ($n = 2$; Fig. 2*S*). However, the distribution of BrdU+/Ki67– cells was strikingly different between wild-type (Fig. 2*O*) and *Ngn2* mutants (Fig. 2*P*). In wild-type cortices, a significant proportion of BrdU+/Ki67– nuclei accumulated in an abventricular band at the border between the VZ and SVZ (Fig. 2*O*), whereas BrdU+/Ki67– nuclei in *Ngn2* mutants were instead scattered throughout the SVZ and IZ (Fig. 2*P*). BrdU+/Ki67– cells in the SVZ/IZ were indeed neurons as many BrdU+ nuclei colabeled with Tuj1 in both wild-type (Fig. 2*Q*) and *Ngn2* mutant (Fig. 2*R*) cortices. Thus, neuronal output was not quantitatively perturbed in *Ngn2* mutants, although there were

qualitative changes with fewer postmitotic neurons remaining in a "holding position" at the VZ/SVZ border.

Misexpression of Mash1 in E14.5 Cortical VZ Progenitors Rapidly Drives Cells Out of the VZ and into the SVZ/IZ

We have previously shown that loss of *Ngn2* results in the upregulation of *Mash1* in cortical progenitors, and that this upregulation partly accounts for the misspecification of *Ngn2* mutant cortical progenitors (Fode and others 2000; Schuurmans and others 2004). We speculated that the alteration in the ratio of apical/basal progenitors in *Ngn2* mutants could similarly arise from the upregulated expression of *Mash1* in *Ngn2* mutant cortical progenitors. Strikingly, at E15.5, the vast majority of the *Ngn2* mutant cortical cells in which Mash1 was ectopically expressed were found in the SVZ, at the border between the VZ/SVZ and in the IZ (Fig. 2*U* vs. *T*), correlating well with the position of the extra nonsurface-dividing progenitors observed in these mutants.

To address directly whether ectopic *Mash1* expression could indeed account for the increased number of VZ progenitors moving into the SVZ/IZ, we used an acute gain-of-function assay. E12.5 (early stage) and E14.5 (intermediate stage) cortical progenitors were electroporated in utero (Saito and Nakatsuji 2001) with a pCIG2-*Mash1* expression construct. The pCIG2 vector (Hand and others 2005) contains an IRES2-EGFP cassette, allowing transfected cells expressing *Mash1* to be detected by EGFP epifluorescence. All fluorescent cells were found to express Mash1 protein upon immunohistochemical analysis (data not shown). We examined the position of GFP-positive cortical cells electroporated with an empty pCIG2 vector (control) and a pCIG2-*Mash1* expression vector 24 h postelectroporation. When compared with control pCIG2 electroporations (Fig. 4*A*,*A*′,*A*′′′,*C*,*C*′,*C*′′′), significantly fewer cells electroporated with pCIG2-*Mash1* (Fig. 4*B*,*B*′,*B*′′′,*D*,*D*′,*D*′′′) remained in the VZ at E12.5 ($P < 0.05$, $n = 3$; Fig. 4*E*) or E14.5 ($P < 0.01$, $n = 3$; Fig. 4*F*). Furthermore, there was a significant increase in the number of *Mash1*-electroporated cells in the SVZ 24 h following the electroporation of E12.5 ($P < 0.05$) and E14.5 ($P < 0.01$) cortices as compared with pCIG2 controls (Fig. 4*E*,*F*). In E14.5–E15.5 experiments, *Mash1*-electroporated cells that

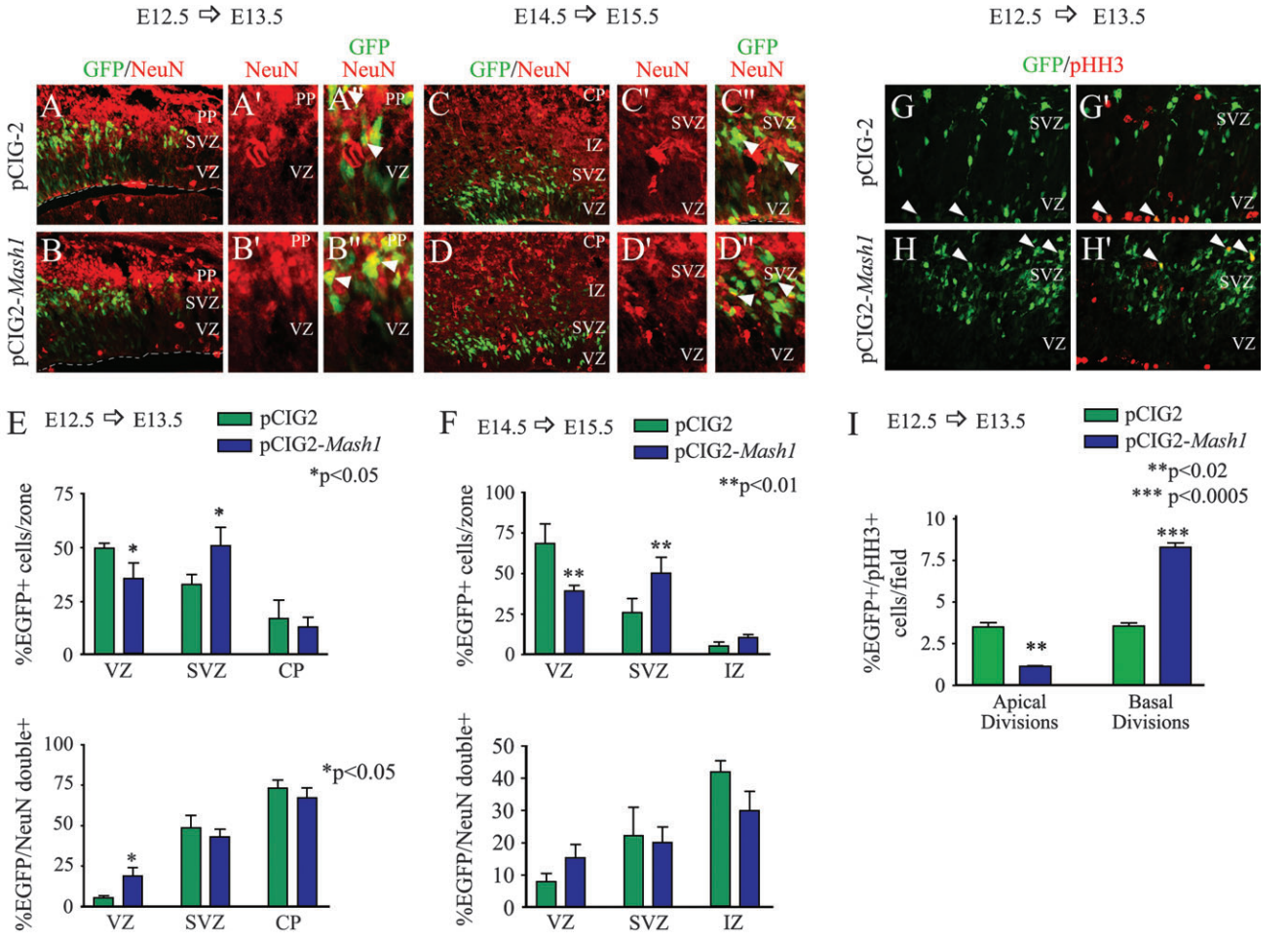

Figure 4. *Mash1* promotes rapid exit from the VZ when misexpressed in cortical progenitors. Electroporation of E12.5 (*A*, *A*′, *A*′′, *B*, *B*′, *B*′′, *G*, *G*′, *H*, *H*′) and E14.5 (*C*, *C*′, *C*′′, *D*, *D*′, *D*′′) cortices with pCIG2 (*A*, *A*′, *A*′′, *C*, *C*′, *C*′′, *G*, *G*′) and pCIG2-*Mash1* (*B*, *B*′, *B*′′, *D*, *D*′, *D*′′, *H*, *H*′) expression vectors (expressing EGFP; green) immunostained with anti-NeuN (red) in (*A*–*D*) and with anti-pHH3 (red) in (*G*–*H*). Arrows in (*A*′′, *B*′′, *C*′′, *D*′′) point to double-labeled cells, representing electroporated cells that differentiated into neurons. Arrows in (*G*, *G*′, *H*, *H*′) point to electroporated progenitors in mitosis. (*E*, *F*) Top graphs show quantification of the percentage of EGFP-expressing cells in each cortical zone 24 h after electroporation of E12.5 (*E*) and E14.5 (*F*) cortices. Bottom graphs show quantification of the percentage of EGFP-positive cells in each zone that differentiated into neurons 24 h following electroporation at E12.5 (*E*) and E14.5 (*F*). (*I*) Quantification of progenitors undergoing apical and basal mitoses (i.e., pHH3-positive) following the electroporation of pCIG2 and pCIG2-*Mash1* constructs. Statistical significance was quantified using Student's *t*-test.

moved into the SVZ/IZ moved significantly farther, almost reaching the CP (Fig. 4*D*), than control electroporated cells (Fig. 4*C*). *Mash1* thus enhanced the movement of cells out of the VZ.

One potential reason why *Mash1* misexpression could promote the movement of cortical VZ progenitors out of the VZ and into the SVZ/IZ is that it exerted its proneural function, promoting cell cycle exit, neuronal differentiation, and migration. To address whether *Mash1*-electroporated cells that had migrated to the SVZ/IZ had begun to differentiate, cortices electroporated at E12.5 and E14.5 with pCIG2 (Fig. 4*A*,*C*) and pCIG2-*Mash1* (Fig. 4*B*,*D*) were labeled with anti-NeuN, a postmitotic neuronal marker. *Mash1* significantly promoted premature neuronal differentiation in the VZ after electroporation at E12.5 ($P < 0.05$; $n = 3$; Fig. 4*E*), but not at E14.5 (Fig. 4*F*). Importantly, there was no significant increase in the number of electroporated cells prematurely acquiring a neuronal fate in the SVZ or IZ, thus indicating that *Mash1* promoted the movement of VZ cells into the SVZ prior to, and independently of, their differentiation and supporting the idea that it acted by promoting the generation of SVZ progenitor cells. To support this conclusion further, cortices electroporated at E12.5 and harvested at E13.5 were immunolabeled with anti-pHH3, allowing us to examine the number of apical and basal progenitors directly. Following the electroporation of *Mash1*, there was a significant increase in the number of EGFP-labeled pHH3+ basal mitoses (8.29 ± 1.02; $P < 0.0005$; $n = 5$; Fig. 4*H*,*H*′,*I*) and a corresponding reduction in EGFP-labeled apical mitoses (1.14 ± 0.23; $P < 0.02$) per field as compared with control pCIG2 electroporations (3.57 ± 0.62 basal, 3.50 ± 0.94 apical; $n = 5$; Fig. 4*G*,*G*′,*I*).

Mash1 Misexpression in the Dorsal Telencephalon Respecifies Early- but Not Mid Stage Cortical Progenitors

We questioned whether ectopic *Mash1* promoted the movement of cortical progenitors from the VZ to the SVZ/IZ as an indirect consequence of its role in misspecifying progenitors from a dorsal to ventral telencephalic identity (Fode and others 2000; Schuurmans and others 2004). To test this possibility, we first performed a molecular analysis of cells in the *Ngn2* mutant SVZ. Notably, all dorsal-specific SVZ markers tested, including *NeuroD*, *Cux2*, *Unc5H4*, and *Sema3c*, were normally expressed in the SVZ of E15.5 *Ngn2* mutants (Supplementary Fig. 1), suggesting that SVZ cells were correctly specified in the absence of Ngn2 and in the presence of ectopic Mash1. We next examined whether any ventral telencephalic markers were ectopically expressed in the *Ngn2* mutant SVZ. *Dlx1*, a homeodomain-encoding gene that is normally expressed in the ventral SVZ and marginal zone at E15.5 (Supplementary Fig. 2*A*,*C*,*C*′) and which we had previously reported to be expressed ectopically in the dorsal preplate and lower CP of *Ngn2* mutants (Fode and others 2000; Schuurmans and others 2004), was also ectopically expressed in the dorsal SVZ of *Ngn2* mutants (Supplementary Fig. 2*B*,*D*,*D*′). In addition, *Id4* an HLH gene expressed in the VZ in the neocortex and in the SVZ of the E15.5 wild-type ventral telencephalon (Supplementary Fig. 2*E*,*E*′) was ectopically expressed in the SVZ and lower CP of *Ngn2* mutants (Supplementary Fig. 2*F*,*F*′). Similarly, *Pax6*, which is normally only expressed in VZ progenitors in the E15.5 neocortex (Supplementary Fig. 2*G*,*G*′,*H*,*H*′) and in postmitotic neurons of dorsal lateral ganglionic eminence origin (Yun and others 2001), was ectopically expressed in the SVZ and in deep-layer CP neurons in *Ngn2* mutants (Supplementary Fig. 2*I*,*I*′,*J*,*J*′). Thus, some cells in the *Ngn2* mutant SVZ, which could be progenitors and/or postmitotic neurons (see below), aberrantly express several ventral telencephalic markers.

We then addressed more directly whether the ability of *Mash1* to promote the movement of cortical progenitors from the VZ to the SVZ was necessarily coupled to the specification of a ventral telencephalic cell fate. For this, we examined whether ectopic expression of *Mash1* by in utero electroporation induced the misspecification of electroporated cells by performing RNA in situ hybridization on cortices that had been electroporated with pCIG2-*Mash1* at E12.5 (Fig. 5*A*–*H*) and E14.5 (Fig. 5*I*–*X*). The electroporated patch on the ipsilateral side of the cortex was identified using *EGFP* (Fig. 5*A*,*I*,*Q*) and *Mash1* (Fig. 5*B*,*J*,*R*) riboprobes. For all markers tested, the contralateral, unelectroporated side is shown to indicate endogenous gene expression. As expected, misexpression of *Mash1* in E12.5 (Fig. 5*C*,*C*′) and E14.5 (Fig. 5*K*,*K*′) cortical progenitors led to ectopic expression of *Delta1*, a known target of the proneural genes. In addition, misexpression of *Mash1* in the dorsolateral cortex at E12.5 induced the ectopic expression of genes that were ectopically expressed in E15.5 *Ngn2* mutants (Supplementary Fig. 2), namely, *Dlx1* (Fig. 5*D*,*D*′), *Id4* (Fig. 5*E*,*E*′), *Pax6* (Fig. 5*F*,*F*′), *Dlx6* (Fig. 5*G*,*G*′), and *GAD1* (Fig. 5*H*,*H*′). In contrast, ectopic expression of *Dlx1* (Fig. 5*L*,*L*′,*T*,*T*′), *Id4* (Fig. 5*M*,*M*′,*U*,*U*′), *Pax6* (Fig. 5*N*,*N*′,*V*,*V*′), *Dlx6* (Fig. 5*O*,*O*′), and *GAD1* transcripts (Fig. 5*P*,*P*′), along with Dlx protein (Fig. *W*,*W*′,*X*,*X*′), was virtually undetectable following *Mash1* misexpression at E14.5 either 24 or 48 h postelectroporation. Indeed, even after 72 h, cortices transfected at E14.5 with pCIG2-*Mash1* failed to express ectopic *Dlx1* (data not shown). Taken together, these results indicated that *Mash1* was much less efficient at respecifying mid stage cortical progenitors, a conclusion we had previously reached from our loss-of-function studies (Schuurmans and others 2004). We thus concluded that ectopic ventral marker expression in the SVZ of E15.5 *Ngn2* mutant cortices likely originated from aberrantly migrating postmitotic neurons that were born several days earlier when upregulated *Mash1* had the capacity to misspecify cortical neurons. Together, these data indicated that the ability of *Mash1* to promote progenitor cell maturation at E14.5 corresponds to a distinct function from its role in cell fate specification.

Discussion

Although it is known that apically dividing progenitor cells in the VZ of the developing neocortex give rise to a secondary pool of progenitor cells that undergo basal cell divisions in the SVZ, the molecular mechanisms guiding this transition remain poorly characterized. In this study, we demonstrate that the proneural genes *Ngn2* and *Mash1* cooperate to regulate the transition of cortical progenitors from apical to basal cell compartments. Strikingly, this requirement for the proneural genes is gradually acquired during development, initially becoming apparent during mid corticogenesis in correlation with the onset of segregated, cell cycle–restricted expression patterns for these proteins in the cortical VZ. Whereas overexpression of *Mash1* misspecifies neurons during early corticogenesis, *Mash1* is sufficient to promote basal cell divisions independently of its role in the specification of neuronal cell fates at later stages. Likewise, *Ngn2* is required to modulate the genesis

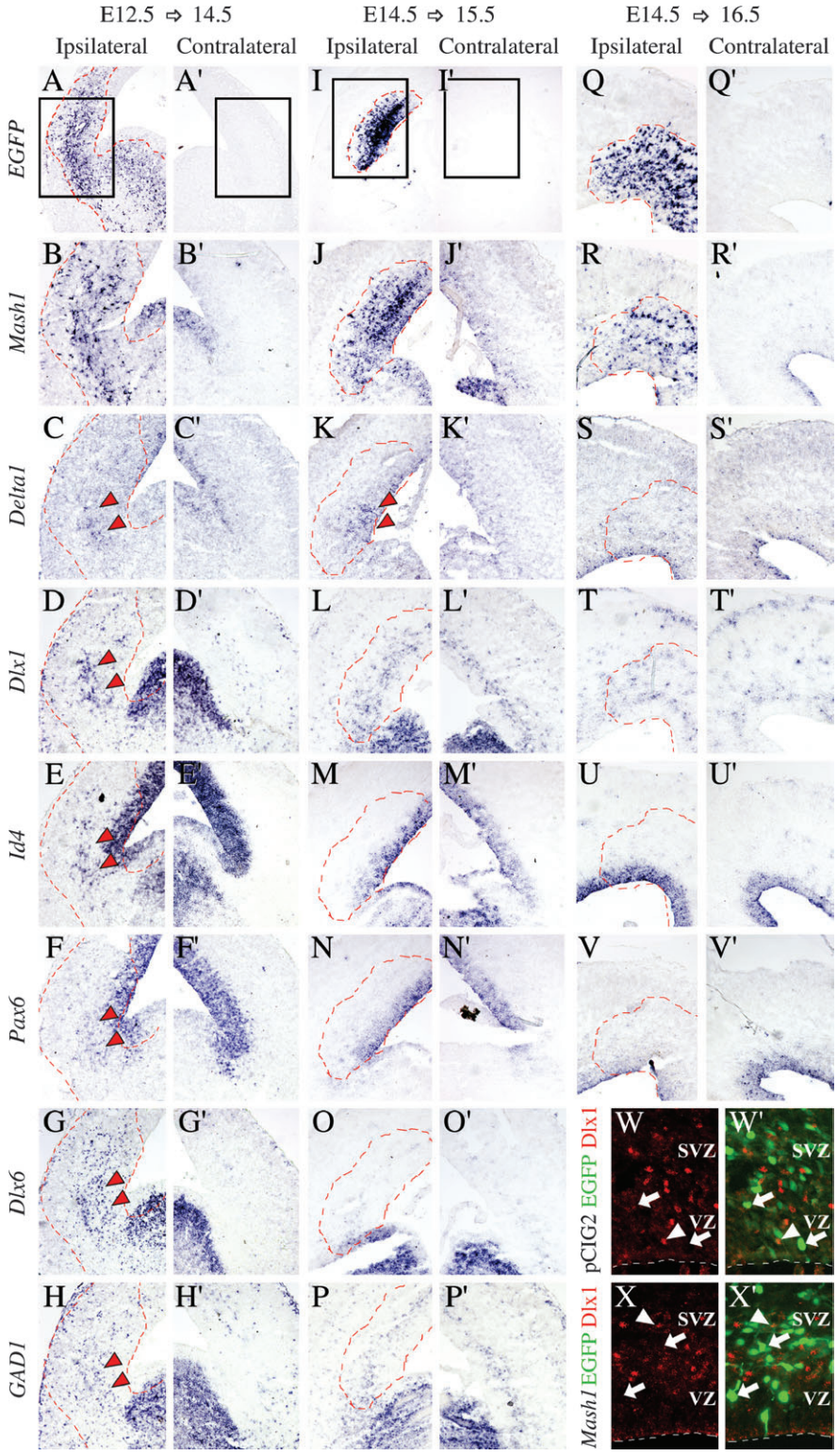

Figure 5. *Mash1* efficiently induces ectopic gene expression in early and not mid stage cortical progenitors. Cortices electroporated with a pCIG2-*Mash1* expression construct at E12.5 were harvested at E14.5 (*A–H*) and cortices electroporated at E14.5 were harvested at E15.5 (*I–P*) or E16.5 (*Q–X*). All electroporated cortices were analyzed for the expression of *EGFP* (*A, A′, I, I′, Q, Q′*), *Mash1* (*B, B′, J, J′, R, R′*), *Delta1* (*C, C′, K, K′, S, S′*), *Dlx1* (*D, D′, L, L′, T, T′*), *Id4* (*E, E′, M, M′, U, U′*), *Pax6* (*F, F′, N, N′, V, V′*), *Dlx6* (*G, G′, O, O′*), and *GAD1* (*H, H′, P, P′*). The electroporated side was designated ipsilateral, and the unelectroporated control side was designated contralateral. The boxed areas in (*A, A′, I, I′*) indicate the areas shown in (*B–H*) and (*J–P*). Electroporated patches on the ipsilateral side are outlined in red. Arrowheads (*A–U*) show ectopic gene expression. Cortices electroporated at E14.5 with the control pCIG2 vector (*W, W′*) or pCIG2-*Mash1* (*X, X′*) were analyzed for Dlx1 protein expression (red; *W, X*) after 48 h. Transfected cells were visualized using EGFP epifluorescence (green, *W′, X′*). Arrowheads, EGFP/Dlx1 double-positive cells, arrows EGFP-positive, Dlx1-negative cells.

of basal progenitors at later stages but is dispensable at early stages. Thus, the proneural genes *Ngn2* and *Mash1* not only function in specifying the identity of early born telencephalic neurons (Casarosa and others 1999; Yun and others 2002; Schuurmans and others 2004) but also have a distinct role in regulating progenitor cell maturation during intermediate-to-late stages of cortical development.

Segregated Expression of Proneural Proteins at Mid corticogenesis

We set out to determine whether a change in expression could underlie changes in proneural gene function during the early *Ngn*-dependent versus mid/late *Ngn*-independent phases of neuronal fate specification in the neocortex. Strikingly, we found that proneural expression profiles were distinct in 2 related respects during early (E12.5) and intermediate (E15.5) stages of corticogenesis. First, although all 3 proneural proteins were coexpressed to a large extent in E12.5 cortical progenitors, they acquired largely complementary expression domains by E15.5. Second, at early stages, cortical progenitors expressing the proneural proteins were randomly distributed throughout the VZ, and hence the cell cycle, contrasting to their clear, cell cycle–biased distribution at E15.5. Specifically, Ngn2 was concentrated in late–G1-phase progenitors, which is consistent with a previous report (Miyata and others 2004). In contrast, Mash1 was expressed in a limited number of VZ progenitors but was not excluded from G2/M- or S-phases of the cell cycle, and within the first gap phase, preferentially accumulated in early G1.

One interpretation of their mutually exclusive expression domains is that Mash1 and Ngn2 are sequentially expressed in the same population of VZ progenitors in early and late G1-phase, respectively. Mechanistically, this could arise due to the ability of *Ngn2* to repress *Mash1* expression (Fode and others 2000). If Ngn2 and Mash1 are indeed expressed in the same lineage in a defined temporal order based on our short-term lineage analysis of GFP expression in $Ngn2^{GFP\text{KI}}$ heterozygotes, which indicates that Ngn2 is expressed in prospective basal progenitors, Mash1 would also be expressed in VZ progenitors committed to a basal cell fate and hence populate the SVZ. However, we cannot rule out an alternative interpretation, which is that Ngn2 and Mash1 are also expressed in distinct progenitor populations at E15.5. Indeed, consistent with the existence of more than one cortical lineage, in previous clonal analyses we showed that *Mash1* plays an essential role in an Ngn2-negative population of cortical progenitors (Nieto and others 2001). Thus, it remains to be determined whether Mash1-positive nuclei in early G1 correspond to self-renewing radial glial cells or to prospective basal progenitors on their way to the SVZ, although our functional experiments strongly favor the latter interpretation.

Proneural Genes Regulate Apical versus Basal Progenitor Cell Divisions in the Neocortex

We reasoned that the segregation of Ngn2 and Mash1 expression in mid corticogenesis would have a functional significance. In this regard, it was particularly noteworthy that Ngn2 was preferentially expressed in the latter half of G1, corresponding to the time when dividing cells make the decision to either exit the cell cycle (i.e., enter G0) or enter another S-phase. However, Ngn2 does not appear to regulate this fate choice, as we did not observe a difference in the Q-fraction, or the number of cells exiting the cell cycle, in *Ngn2* mutant cortices. Instead, the distribution of newly differentiated neurons was altered, as these cells failed to temporally halt at the VZ/SVZ border and instead rapidly migrated into the IZ and CP in *Ngn2* mutants. Thus, the waiting period that had been previously observed for SVZ precursors and/or their postmitotic neuronal daughters (Bayer and others 1991; Noctor and others 2004; Zimmer and others 2004) requires *Ngn2* activity.

How do we reconcile our expression data, whereby Ngn2 is expressed by future basal progenitors committed to leaving the VZ, and our functional data, which indicates that the loss of *Ngn2* results in excessive basal cell divisions, suggesting that it normally prevents basal and promotes apical cell divisions? Our model is that at early stages, *Ngn2* would promote the differentiation of VZ progenitor daughters, which would then exit the VZ, pause at the VZ/SVZ border, transit through the SVZ, and enter the CP as postmitotic neurons. Indeed, *Ngn2* is required to specify neuronal phenotypes at early stages of corticogenesis (Schuurmans and others 2004), when neurons are thought to be derived mainly from asymmetric divisions at the surface of the VZ that generate one neuron and one progenitor daughter (Chenn and McConnell 1995; Haubensak and others 2004; Kosodo and others 2004; Miyata and others 2004). At later stages, when *Ngn2* is dispensable for neuronal subtype specification and progenitor divisions are increasingly symmetric and neurogenic (Haubensak and others 2004; Kosodo and others 2004; Miyata and others 2004; Noctor and others 2004), *Ngn2* would instead modulate the behavior of VZ progenitors both positively, by promoting progenitor cell maturation as indicated by Miyata and others (2004) and supported by our short-term lineage tracing data, and negatively, by partially suppressing a faster/more potent *Mash1*-mediated pathway. Thus, by having both positive and negative functions, *Ngn2* would not only permit progenitor maturation but also act as a brake to ensure that maturation did not exhaust VZ progenitors either altogether or too quickly. What is our evidence for this model? First, in *Ngn2* mutants we observed a significant increase in dividing cells in the SVZ/IZ at the expense of VZ progenitors, which led to a near complete depletion of the VZ by E18.5 in *Ngn1;Ngn2* double mutants (data not shown). Second, ectopic Mash1-expressing cells in *Ngn2* mutants preferentially localized to the SVZ/IZ. Finally, in our gain-of-function experiments, misexpression of *Mash1* enhanced the migration of VZ progenitors into the SVZ/IZ where they stalled for 24–48 h before differentiating and entering the CP (data not shown).

In potential conflict with our model, *Mash1* misexpression had the capacity to promote progenitor maturation or movement into the SVZ even at early stages (i.e., E12.5), whereas supernumerary SVZ mitoses were only detected at later stages of corticogenesis in *Ngn2* mutants. However, there is a major difference between these 2 experiments. In our loss-of-function model, we examined basal cell divisions in the entire cortical progenitor population, presumably including those progenitors that did not express *Mash1*, which possibly dilutes out any effect of ectopic *Mash1* expression. In contrast, in our gain-of-function studies, we focused exclusively on the behavior of progenitors that misexpressed *Mash1*. The gradual increase in basal mitoses in *Ngn2* mutants between E12.5 and E15.5 could thus reflect a cumulative effect rather than time-dependent functional differences. Alternatively, the ability of *Mash1* to promote nonsurface divisions could be much more potent at

later versus early stages of cortical development. Although we have not directly compared early and late electroporations with respect to progenitor cell maturation, there is a clear difference between the early and late activities of *Mash1* in cell fate specification. This suggests that the transcriptional cascade activated by *Mash1* differs considerably during these periods.

Molecular Pathways Downstream of Mash1

How does *Mash1* promote progenitor cell maturation in the neocortex? In the ventral telencephalon of *Mash1* mutants, VZ progenitors ectopically/precociously express SVZ markers, including the *Dlx* genes, leading Yun and others (2002) and Casarosa and others (1999) to conclude that *Mash1* was required for maintaining the VZ identity of ventral progenitors. Yet, leukemia inhibitory factor/ciliary neurotrophic factor, which has recently been shown to be required to maintain VZ stem cells, appears to act through *Notch1* to suppress *Mash1* expression (Chojnacki and others 2003; Gregg and Weiss 2005). An alternative possibility that would reconcile these data and our own is that *Mash1* is instead required to direct the movement of maturing progenitors out of the VZ and into the SVZ. To draw a parallel with *Drosophila* neural selection, the most immediate effects of proneural gene activation are upregulation of *Delta*, followed by delamination and migration out of the ectodermal epithelium (Bertrand and others 2002). Likewise, a significant proportion of the genes most rapidly induced by the bHLH transcription factor *MyoD* are involved in cellular adhesion and extracellular matrix remodeling, suggesting that the immediate function of bHLH genes might be to activate cellular migration (Bergstrom and others 2002; Tapscott 2005). Thus, although we have not identified *Mash1* target genes that could mechanistically account for *Mash1*-mediated progenitor maturation, it is interesting to speculate that *Mash1* regulates this process by directly activating progenitor cell migration.

Mash1 has previously been shown to have a dual function in the embryonic telencephalon, the promotion of neurogenesis, and the specification of a ventral telencephalic neuronal identity. Our ectopic expression experiments demonstrate that the ability of *Mash1* to promote the movement of cortical progenitors from the VZ into the SVZ occurred without a concomitant induction of *Dlx*, *Pax6*, or *Id4* expression at E14.5, although *Delta1* could still be induced. This suggests that the ability of *Mash1* to promote progenitor cell maturation is independent from its ability to specify cell fates. Indeed, a role for neocortical *Mash1* in transactivating genes such as *Dlx1* and *GAD1*, which are associated with γ-aminobutyric acidergic (GABAergic) neurogenesis, in the neocortex would conflict with numerous investigations that have shown little to no GABAergic neurogenesis from murine neocortical progenitors (Anderson and others 1997, 1999, 2002; Tan and others 1998), although *Mash1* has been shown to contribute to GABAergic neurogenesis in the human neocortical primordium (Letinic and others 2002). Thus, although *Mash1* has the ability to specify GABAergic neuronal fates at early stages, we suggest that this activity is almost entirely masked by *Ngn1* and *Ngn2*, which we show here are initially highly coexpressed with *Mash1*. At later stages, neither *Ngn2* nor *Mash1* appears to be capable of specifying cell fates (this study and Schuurmans and others 2004).

In summary, our data reveal a novel role for the proneural genes *Ngn2* and *Mash1* in regulating the mode of cell division by radial glial cells located in the cortical VZ, a function that is distinct from their role in the specification of cortical neuronal identities.

Supplementary Material

Supplementary material can be found at: http://www.cercor.oxfordjournals.org/.

Notes

We thank Eva Hadzimova for establishing in utero technology in the lab of CS and N. Klenin for assistance with sectioning and RNA in situ hybridization. We also thank Grace Panganiban, Jane Johnson, Masato Nakafuku, and David Anderson for antisera and C. Logan for a GFP riboprobe. This work was supported by Canadian Institutes of Health Research (CIHR) Operating Grant MOP 44094 to CS, by grants from the European Community Research and Technological Development program (QLG3-CT-2000-01471), the Human Frontier Science Program, the Association pour la Recherche sur le Cancer, and the action thématique concertée reseau cellules souche neurales from Institut National de la Santé et de la Recherche Médicale (INSERM) to FG, and by institutional funds from INSERM, Centre National de la Recherche Scientifique, and Hôpital Universitaire de Strasbourg (at Institut de Génétique et Biologie Moléculaire et Cellulaire), and from the Medical Research Council (at National Institute of Medical Research). CS is a CIHR New Investigator and Alberta Heritage Foundation for Medical Research (AHFMR) scholar. OB is supported by a MRC studentship, PM by a CIHR Canada Graduate Scholarship and an AHFMR Studentship, LN by a European Molecular Biology Organization postdoctoral fellowship, and L-ML by a CIHR training grant in Genetics, Child Development and Health. *Conflict of Interest*: None declared.

Address correspondence to Carol Schuurmans, Department of Biochemistry and Molecular Biology, Institute of Maternal and Child Health, University of Calgary, Calgary, Alberta, Canada. Email: cschuurm@ucalgary.ca, fguille@nimr.mrc.ac.uk.

References

Anderson S, Mione M, Yun K, Rubenstein JL. 1999. Differential origins of neocortical projection and local circuit neurons: role of Dlx genes in neocortical interneuronogenesis. Cereb Cortex 9:646–654.

Anderson SA, Eisenstat DD, Shi L, Rubenstein JL. 1997. Interneuron migration from basal forebrain to neocortex: dependence on Dlx genes. Science 278:474–476.

Anderson SA, Kaznowski CE, Horn C, Rubenstein JL, McConnell SK. 2002. Distinct origins of neocortical projection neurons and interneurons in vivo. Cereb Cortex 12:702–709.

Anthony TE, Klein C, Fishell G, Heintz N. 2004. Radial glia serve as neuronal progenitors in all regions of the central nervous system. Neuron 41:881–890.

Bayer SA, Altman J, Russo RJ, Dai XF, Simmons JA. 1991. Cell migration in the rat embryonic neocortex. J Comp Neurol 307:499–516.

Behar T, Ma W, Hudson L, Barker JL. 1994. Analysis of the anatomical distribution of GAD67 mRNA encoding truncated glutamic acid decarboxylase proteins in the embryonic rat brain. Brain Res Dev Brain Res 77:77–87.

Bergstrom DA, Penn BH, Strand A, Perry RL, Rudnicki MA, Tapscott SJ. 2002. Promoter-specific regulation of MyoD binding and signal transduction cooperate to pattern gene expression. Mol Cell 9:587–600.

Bertrand N, Castro DS, Guillemot F. 2002. Proneural genes and the specification of neural cell types. Nat Rev Neurosci 3:517–530.

Brazel CY, Romanko MJ, Rothstein RP, Levison SW. 2003. Roles of the mammalian subventricular zone in brain development. Prog Neurobiol 69:49–69.

Casarosa S, Fode C, Guillemot F. 1999. Mash1 regulates neurogenesis in the ventral telencephalon. Development 126:525–534.

Cau E, Gradwohl G, Fode C, Guillemot F. 1997. Mash1 activates a cascade of bHLH regulators in olfactory neuron progenitors. Development 124:1611–1621.

Caviness VS Jr. 1982. Neocortical histogenesis in normal and reeler mice: a developmental study based upon [3H]thymidine autoradiography. Brain Res 256:293–302.
Caviness VS Jr, Takahashi T, Nowakowski RS. 1995. Numbers, time and neocortical neuronogenesis: a general developmental and evolutionary model. Trends Neurosci 18:379–383.
Chenn A, McConnell SK. 1995. Cleavage orientation and the asymmetric inheritance of Notch1 immunoreactivity in mammalian neurogenesis. Cell 82:631–641.
Chiasson BJ, Tropepe V, Morshead CM, van der Kooy D. 1999. Adult mammalian forebrain ependymal and subependymal cells demonstrate proliferative potential, but only subependymal cells have neural stem cell characteristics. J Neurosci 19: 4462–4471.
Chojnacki A, Shimazaki T, Gregg C, Weinmaster G, Weiss S. 2003. Glycoprotein 130 signaling regulates Notch1 expression and activation in the self-renewal of mammalian forebrain neural stem cells. J Neurosci 23:1730–1741.
Fode C, Ma Q, Casarosa S, Ang SL, Anderson DJ, Guillemot F. 2000. A role for neural determination genes in specifying the dorsoventral identity of telencephalic neurons. Genes Dev 14:67–80.
Gradwohl G, Fode C, Guillemot F. 1996. Restricted expression of a novel murine atonal-related bHLH protein in undifferentiated neural precursors. Dev Biol 180:227–241.
Gregg C, Weiss S. 2005. CNTF/LIF/gp130 receptor complex signaling maintains a VZ precursor differentiation gradient in the developing ventral forebrain. Development 132:565–578.
Hand R, Bortone D, Mattar P, Nguyen L, Heng JL, Guerrier S, Boutt E, Peters E, Barnes AP, Parras C, Schuurmans C, Guillemot F, Polleux F. 2005. Phosphorylation of neurogenin2 specifies the migration properties and the dendritic morphology of pyramidal neurons in the neocortex. Neuron 48:45–62.
Haubensak W, Attardo A, Denk W, Huttner WB. 2004. Neurons arise in the basal neuroepithelium of the early mammalian telencephalon: a major site of neurogenesis. Proc Natl Acad Sci USA 101: 3196–3201.
Ishii Y, Nakamura S, Osumi N. 2000. Demarcation of early mammalian cortical development by differential expression of fringe genes. Brain Res Dev Brain Res 119:307–320.
Kakita A, Goldman JE. 1999. Patterns and dynamics of SVZ cell migration in the postnatal forebrain: monitoring living progenitors in slice preparations. Neuron 23:461–472.
Kosodo Y, Roper K, Haubensak W, Marzesco AM, Corbeil D, Huttner WB. 2004. Asymmetric distribution of the apical plasma membrane during neurogenic divisions of mammalian neuroepithelial cells. EMBO J 23:2314–2324.
Kriegstein AR, Noctor SC. 2004. Patterns of neuronal migration in the embryonic cortex. Trends Neurosci 27:392–399.
Letinic K, Zoncu R, Rakic P. 2002. Origin of GABAergic neurons in the human neocortex. Nature 417:645–649.
Levison SW, Goldman JE. 1993. Both oligodendrocytes and astrocytes develop from progenitors in the subventricular zone of postnatal rat forebrain. Neuron 10:201–212.
Lindsell CE, Boulter J, DiSibio G, Gossler A, Weinmaster G. 1996. Expression patterns of Jagged, Delta1, Notch1, Notch2, and Notch3 genes identify ligand-receptor pairs that may function in neural development. Mol Cell Neurosci 8:14–27.
Lois C, Alvarez-Buylla A. 1993. Proliferating subventricular zone cells in the adult mammalian forebrain can differentiate into neurons and glia. Proc Natl Acad Sci USA 90:2074–2077.
Ma Q, Chen Z, del Barco Barrantes I, de la Pompa JL, Anderson DJ. 1998. Neurogenin1 is essential for the determination of neuronal precursors for proximal cranial sensory ganglia. Neuron 20:469–482.
Ma Q, Sommer L, Cserjesi P, Anderson DJ. 1997. Mash1 and neurogenin1 expression patterns define complementary domains of neuroepithelium in the developing CNS and are correlated with regions expressing notch ligands. J Neurosci 17:3644–3652.
Malatesta P, Hack MA, Hartfuss E, Kettenmann H, Klinkert W, Kirchhoff F, Gotz M. 2003. Neuronal or glial progeny: regional differences in radial glia fate. Neuron 37:751–764.
Mattar P, Britz O, Johannes C, Nieto M, Ma L, Rebeyka A, Klenin N, Polleux F, Guillemot F, Schuurmans C. 2004. A screen for downstream effectors of Neurogenin2 in the embryonic neocortex. Dev Biol 273:373–389.
Miyata T, Kawaguchi A, Saito K, Kawano M, Muto T, Ogawa M. 2004. Asymmetric production of surface-dividing and non-surface-dividing cortical progenitor cells. Development 131:3133–3145.
Miyata T, Maeda T, Lee JE. 1999. NeuroD is required for differentiation of the granule cells in the cerebellum and hippocampus. Genes Dev 13:1647–1652.
Nieto M, Monuki ES, Tang H, Imitola J, Haubst N, Khoury SJ, Cunningham J, Gotz M, Walsh CA. 2004. Expression of Cux-1 and Cux-2 in the subventricular zone and upper layers II–IV of the cerebral cortex. J Comp Neurol 479:168–180.
Nieto M, Schuurmans C, Britz O, Guillemot F. 2001. Neural bHLH genes control the neuronal versus glial fate decision in cortical progenitors. Neuron 29:401–413.
Noctor SC, Flint AC, Weissman TA, Dammerman RS, Kriegstein AR. 2001. Neurons derived from radial glial cells establish radial units in neocortex. Nature 409:714–720.
Noctor SC, Martinez-Cerdeno V, Ivic L, Kriegstein AR. 2004. Cortical neurons arise in symmetric and asymmetric division zones and migrate through specific phases. Nat Neurosci 7:136–144.
Reynolds BA, Weiss S. 1992. Generation of neurons and astrocytes from isolated cells of the adult mammalian central nervous system. Science 255:1707–1710.
Saito T, Nakatsuji N. 2001. Efficient gene transfer into the embryonic mouse brain using in vivo electroporation. Dev Biol 240: 237–246.
Sauer ME, Walker BE. 1959. Radioautographic study of interkinetic nuclear migration in the neural tube. Proc Soc Exp Biol Med 101:557–560.
Schuurmans C, Armant O, Nieto M, Stenman JM, Britz O, Klenin N, Langevin L-M, Seibt J, Brown C, Tang H, Cunningham JM, Dyck R, Walsh C, Campbell K, Polleux F, Guillemot F. 2004. Sequential phases of cortical specification involve Neurogenin-dependent and-independent pathways. EMBO J 23:2892–2902.
Seibt J, Schuurmans C, Gradwhol G, Dehay C, Vanderhaeghen P, Guillemot F, Polleux F. 2003. Neurogenin2 specifies the connectivity of thalamic neurons by controlling axon responsiveness to intermediate target cues. Neuron 39:439–452.
Sidman RL, Miale IL, Feder N. 1959. Cell proliferation and migration in the primitive ependymal zone: an autoradiographic study of histogenesis in the nervous system. Exp Neurol 1:322–333.
Sidman RL, Rakic P. 1973. Neuronal migration, with special reference to developing human brain: a review. Brain Res 62:1–35.
Smart IH, Dehay C, Giroud P, Berland M, Kennedy H. 2002. Unique morphological features of the proliferative zones and postmitotic compartments of the neural epithelium giving rise to striate and extrastriate cortex in the monkey. Cereb Cortex 12:37–53.
Smart IH, McSherry GM. 1982. Growth patterns in the lateral wall of the mouse telencephalon. II. Histological changes during and subsequent to the period of isocortical neuron production. J Anat 134(Pt 3):415–442.
Stoykova A, Treichel D, Hallonet M, Gruss P. 2000. Pax6 modulates the dorsoventral patterning of the mammalian telencephalon. J Neurosci 20:8042–8050.
Takahashi T, Goto T, Miyama S, Nowakowski RS, Caviness VS Jr. 1999. Sequence of neuron origin and neocortical laminar fate: relation to cell cycle of origin in the developing murine cerebral wall. J Neurosci 19:10357–10371.
Takahashi T, Nowakowski RS, Caviness VS Jr. 1995. The cell cycle of the pseudostratified ventricular epithelium of the embryonic murine cerebral wall. J Neurosci 15:6046–6057.
Tan SS, Kalloniatis M, Sturm K, Tam PP, Reese BE, Faulkner-Jones B. 1998. Separate progenitors for radial and tangential cell dispersion during development of the cerebral neocortex. Neuron 21:295–304.
Tapscott SJ. 2005. The circuitry of a master switch: Myod and the regulation of skeletal muscle gene transcription. Development 132:2685–2695.

Tarabykin V, Stoykova A, Usman N, Gruss P. 2001. Cortical upper layer neurons derive from the subventricular zone as indicated by Svet1 gene expression. Development 128:1983–1993.

Weissman T, Noctor SC, Clinton BK, Honig LS, Kriegstein AR. 2003. Neurogenic radial glial cells in reptile, rodent and human: from mitosis to migration. Cereb Cortex 13:550–559.

Yun K, Fischman S, Johnson J, Hrabe de Angelis M, Weinmaster G, Rubenstein JL. 2002. Modulation of the notch signaling by Mash1 and Dlx1/2 regulates sequential specification and differentiation of progenitor cell types in the subcortical telencephalon. Development 129:5029–5040.

Yun K, Potter S, Rubenstein JL. 2001. Gsh2 and Pax6 play complementary roles in dorsoventral patterning of the mammalian telencephalon. Development 128:193–205.

Zerlin M, Levison SW, Goldman JE. 1995. Early patterns of migration, morphogenesis, and intermediate filament expression of subventricular zone cells in the postnatal rat forebrain. J Neurosci 15:7238–7249.

Zimmer C, Tiveron MC, Bodmer R, Cremer H. 2004. Dynamics of Cux2 expression suggests that an early pool of SVZ precursors is fated to become upper cortical layer neurons. Cereb Cortex 14: 1408–1420.